Y-Shaped Ligand-Driven Gold Nanoparticles for Highly Efficient Tumoral Uptake and Photothermal Ablation

Ung Yeol Lee,[†] Yu Seok Youn,[‡] Jeyoung Park,[§] and Eun Seong Lee*,[†]

[†]Department of Biotechnology, The Catholic University of Korea, 43-1 Yeokgok 2-dong, Wonmi-gu, Bucheon, Gyeonggi-do 420-743, Republic of Korea, [‡]College of Pharmacy, SungKyunKwan University, 300 Chonchon-dong, Jangan-ku, Suwon, Gyeonggi-do 440-746, Republic of Korea, and [§]Research Center for Industrial Chemical Biotechnology, Ulsan Division of Chemical R&BD, Korea Research Institute of Chemical Technology (KRICT), Ulsan 681-802, Republic of Korea

ABSTRACT We report functional gold nanoparticles (AuNP) with antibody-like ligands. These particles consist of Y-shaped ligands and AuNP. Transferrin (Tf) and Tat peptide were linked to each head of a Y-shaped poly(ethylene glycol) (PEG)-containing dopamine at one tail site. Also, Y-shaped ligands (with Tf and Tat peptide) were anchored to the surface of the AuNP as the result of noncovalent conjugation of dopamine and the AuNP. Interestingly, the partial shielding of Tat peptides by large Tf molecules rather improved Tf-mediated endocytosis of the AuNP, while minimizing the natural nonspecific cell interaction of Tat peptides. This system resulted in highly improved *in vitro*/*in vivo* tumor-selective uptake over AuNP bearing a single ligand (Tf or Tat peptides). Furthermore, this system resulted in significant enhancement of *in vivo* photothermal tumor cell ablation under light-irradiation conditions for AuNP. We believe that this design is a promising method to easily modify conventional antibodies or ligands to improve their disease-recognition ability.

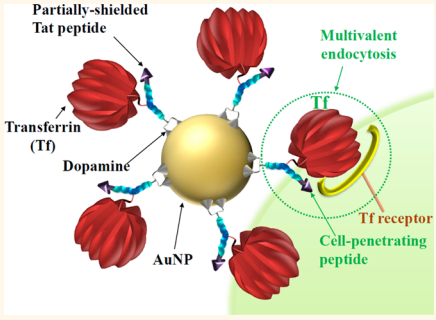

KEYWORDS: Y-shaped ligands · gold nanoparticles · Tat peptide · transferrin · photothermal ablation

Unique encoding of tailor-made antibodies or ligands on bioactive substances has resulted in significant progress in the development of biopharmaceutical technologies.[1−3] In particular, nanosized particles encoded with antibodies or ligands have received a great deal of attention because of their paired cell-specific interactions (such as antigen/antibody and ligand/receptor) and their ability to serve as scaffolds for therapeutic payloads.[4−7] Over the past 20 years, nanosized particles paired with suitable drugs (or imaging agents) and antibodies (or ligands) have been extensively utilized for disease treatment (or diagnosis) after passive and active diffusion in the body.[4−7] The dream of a "magic bullet" in targeted disease therapy has become of great interest in the pharmaceutical and biotechnological fields.[1−7]

Notably, recent research efforts have been focused on creating nanoparticle systems bearing functional antibodies or ligands for highly efficient tumor treatment and diagnosis.[4,5,8,9] These approaches are predicated on the premise that use of the nanoparticles with well-constructed antibodies or ligands will result in pronounced improvement in tumor internalization and tumor therapy. However, the limited functionality and unsatisfactory tumoral uptake of nanoparticles with conventional antibodies or ligands usually result in relatively low effectiveness because of practical difficulties in overcoming obstacles in natural *in vivo* conditions.[3,5,10] Despite recent technological attempts to modify conventional antibodies or ligands through genetic/chemical modifications or phage display peptide libraries, there have been few examples of nanoparticles coupled with precisely reconstructed antibodies or ligands.[1−5,8−10]

In this study, we report gold nanoparticles (AuNP) with unique Y-shaped ligands and encodable structural identities. As shown in Figure 1a, the Y-shaped ligands mimicking

* Address correspondence to eslee@catholic.ac.kr.

Received for review November 10, 2014 and accepted December 2, 2014.

Published online December 02, 2014
10.1021/nn506411q

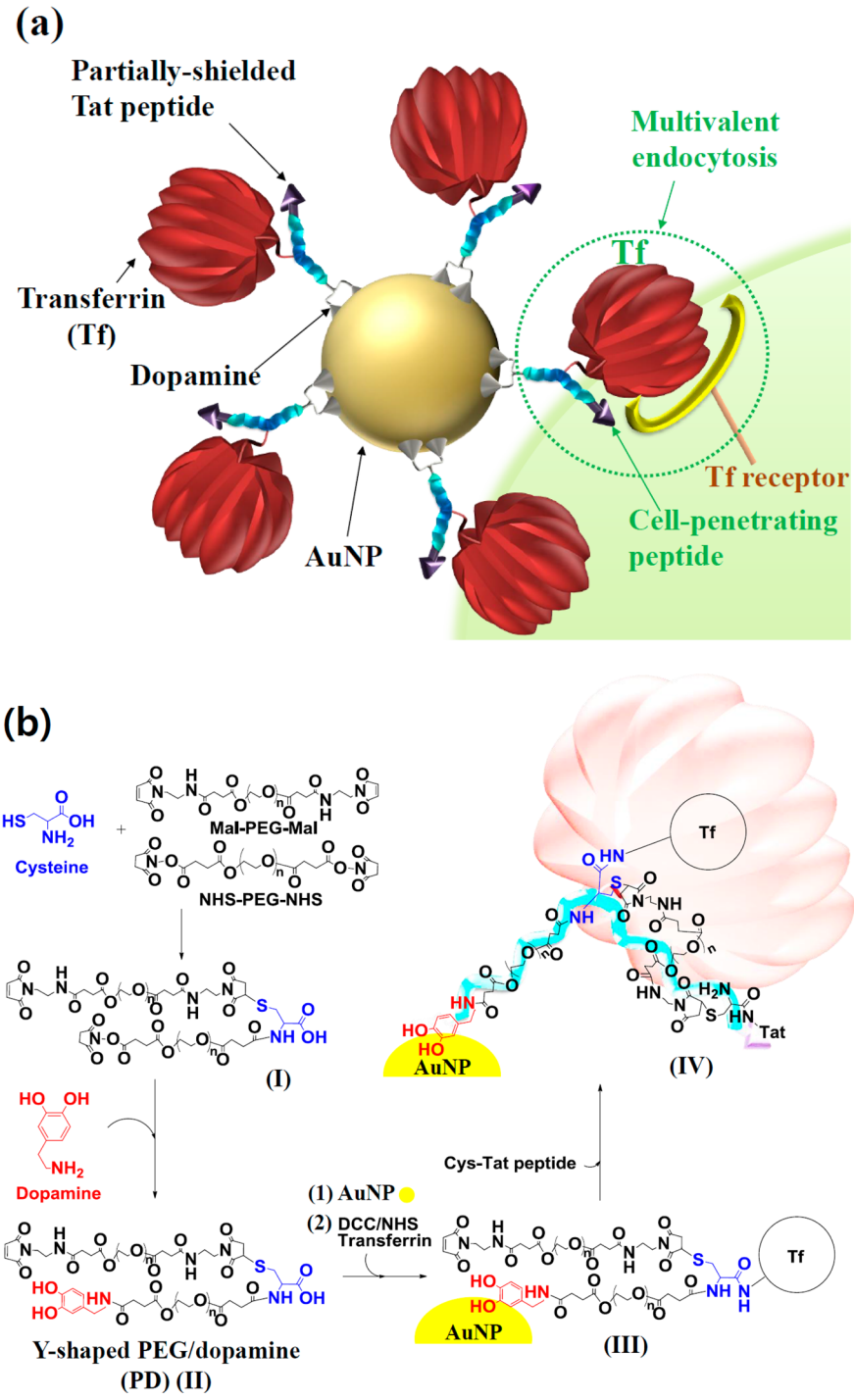

Figure 1. (a) Schematic concept of multivalent endocytosis using antibody-like ligand-bearing AuNP. See the text for more details. (b) Synthesis scheme for the antibody-like ligand-bearing AuNP.

the shape of an antibody consist of a transferrin [Tf, M_w 80 kDa, a target protein for Tf receptor (TfR)-positive tumor cells],[11] Tat peptide,[12] poly(ethylene glycol) (PEG), and dopamine (a high-affinity anchor for AuNP and a hydrophobic shell[13]) (Figure 1a). Here, we prepared Y-shaped ligands after generating a Y-shaped PEG using cysteine and difunctionalized PEG and conjugating with dopamine, Tat peptide, and Tf. Briefly, the terminal *N*-hydroxysuccinimide (NHS) moiety of the Y-shaped PEG (**I**) [prepared after the chemical reaction of cysteine (as a chemical bridge) with maleimide (Mal)-difunctionalized PEG (Mal-PEG-Mal) and NHS-difunctionalized PEG (NHS-PEG-NHS)] reacted with the free amine group of dopamine, producing a Y-shaped PEG containing dopamine (Y-shaped PEG/dopamine: PD, **II**) (Figure 1b). Next, a sticky dopamine tail was bound to the surface of AuNP (stabilized using excess dodecanethiol,[14] particle size

in diameter = 10 nm in choroform, 50−70 nm in phosphate-buffered saline (PBS) (data not shown)] *via* noncovalent binding,[13] producing PD-bearing AuNP (PD-AuNP) (Figure 1b). The terminal carboxylic acid group of PD-AuNP was preactivated using *N,N′*-dicyclohexylcarbodiimide (DCC) and NHS and then chemically reacted with Tf, producing PD-AuNP with Tf (Tf-PD-AuNP, **III**) (Figure 1b). The terminal Mal moiety of Tf-PD-AuNP reacted with the thiol group of the Tat peptide [with terminal cysteine (Cys)], producing PD-AuNP with Tf and Tat (Tf/Tat-PD-AuNP, **IV**) (Figure 1b). As a result, Tat peptides and Tf were chemically encoded to each head of the Y-shaped PEG linked to AuNP.

RESULTS AND DISCUSSION

We anticipated that the presence of two targeting moieties would provide a promising route for multivalent endocytosis (TfR-mediated[11,15] and Tat-mediated endocytosis[5,12]) (Figure 1a). In particular, we hypothesized that Tat peptides (partially shielded by large Tf molecules) could serve as a biological catalyst to improve the cell-binding affinity of Tf (Figure 1a).

We prepared various combinations of AuNP (PD-AuNP, Tf-PD-AuNP, Tat-PD-AuNP, and Tf/Tat-PD-AuNP) as listed in Table 1. We also calculated the weight fractions of PD, Tf, and Tat in AuNP after measuring the concentration of free PD, free Tf, and free Tat remaining in the supernatant obtained after ultracentrifugation of the AuNP solution at 25 000 rpm for 10 min (Table 1 and Supporting Information). Averages of 2.28−2.30% PD, 0.20−021% Tf, and 0.39−0.40% Tat were embedded in AuNP (Table 1). The images obtained from a transmission electron microscope (TEM) illustrate that each AuNP (average diameter of 50−100 nm) was almost spherical (Figure 2a). In addition, the zeta-potential of PD-AuNP was −3.3 mV. The zeta-potential of AuNP changed from −2.2 mV (Tat-PD-AuNP) to −3.1 mV (Tf/Tat-PD-AuNP) with respect to the presence or absence of positive-charged Tat peptides and negative-charged Tf (Table 1).

Next, to evaluate whether the Y-shaped ligands could indeed improve the cellular uptake of AuNP, we first performed *in vitro* cell imaging studies using MDA-MB-231 (TfR-positive)[11] or CHO-K1 (TfR-negative)[15] cells. Figure 2b shows confocal images of MDA-MB-231 (TfR-positive) cells treated using fluorescent chlorin e6 (Ce6) dye-labeled AuNP at 37 °C for 4 h. Here, the fluorescent Ce6 dye[16,17] was chemically conjugated with dopamine and then embedded to the surface of AuNP through noncovalent conjugation[13] of dopamine and AuNP. We stained the cells using 4′,6-diamidino-2-phenylindole dihydrochloride (DAPI) and wheat germ agglutinin (WGA)-Alexa Fluor 488 to visualize the cell nuclei and membranes,[16] respectively. The confocal images revealed the highest cellular uptake of Tf/Tat-PD-AuNP and Tat-PD-AuNP (Figure 2b). Ce6 fluorescence[16] of Tf/Tat-PD-AuNP and Tat-PD-AuNP was primarily observed in the cytoplasm (or perinuclear region), reflecting their efficient cellular internalization. In contrast, Tf-PD-AuNP showed relatively poor fluorescence in MDA-MB-231 cells under the same experimental conditions. In addition, no apparent fluorescent intensity was noted for PD-AuNP (Figure 2b).

TABLE 1. Manufacturing Conditions and Characterization of Y-Shaped Ligand-Bearing AuNP

	weight fraction (%) of PD, Tf, and Tat in nanoparticles			
sample	PD	Tf	Tat	zeta-potential (mV)
PD-AuNP	2.30			−3.3 ± 0.2
Tf-PD-AuNP	2.30	0.21		−4.1 ± 0.1
Tat-PD-AuNP	2.29		0.40	−2.2 ± 0.4
Tf/Tat-PD-AuNP	2.28	0.20	0.39	−3.1 ± 0.1

It is interesting to note that unlike the strong fluorescence of Tf/Tat-PD-AuNP observed in TfR-positive MDA-MB-231 cells (Figure 2b), no apparent fluorescent intensity of Tf/Tat-PD-AuNP in the TfR-negative CHO-K1 cells was observed (Figure 2c). However, Tat-PD-AuNP was still internalized by TfR-negative CHO-K1 cells (Figure 2c), probably due to the nonspecific cell-penetrating ability of the Tat peptide alone. It is known that Tat peptide-conjugated macromolecules are extensively internalized by cells *via* nonspecific pinocytosis after electrostatic interactions with cellular membranes.[5,12] Our results indicate that Tf/Tat-PD-AuNP inhibits the independent cell penetration of the Tat peptide (probably due to the steric hindrance of the large Tf molecule located near the Tat peptide) but enhances TfR-mediated endocytosis. We believe that multivalent endocytosis (the TfR-mediated endocytosis[11] and the following Tat peptide-mediated cellular interaction[12]) causes the improved tumor-selective uptake of AuNP.

Figure 2d also evidences the extensive internalization of Tf/Tat-PD-AuNP. The uptake of Tf/Tat-PD-AuNP by the MDA-MB-231 cells was significantly increased, compared with those of Tf-PD-AuNP and PD-AuNP, as measured using inductively coupled plasma mass spectrometry (ICP-MS).[18] The TEM images (Figure 2e) revealed that Tf/Tat-PD-AuNP in the endosomes was actively transferred to the cytoplasm of MDA-MB-231 cells, although Tf/Tat-PD-AuNP did not interact with CHO-K1 cells. In addition, Tf-PD-AuNP exhibited relatively low cell binding by the MDA-MB-231 cells during a short treatment (incubation) time (1 h), although Tf-PD-AuNP has Tf on the surface of the AuNP. Figure 2f shows the quantitative results of the cellular uptake of Ce6 dye-labeled AuNP using a FACSCalibur flow cytometer. The average fluorescence intensity of Tf/Tat-PD-AuNP was ~9.05×10^3, and that of Tf-PD-AuNP was ~383. Taken together, the data demonstrated the high uptake of Tf/Tat-PD-AuNP in MDA-MB-231 cells.

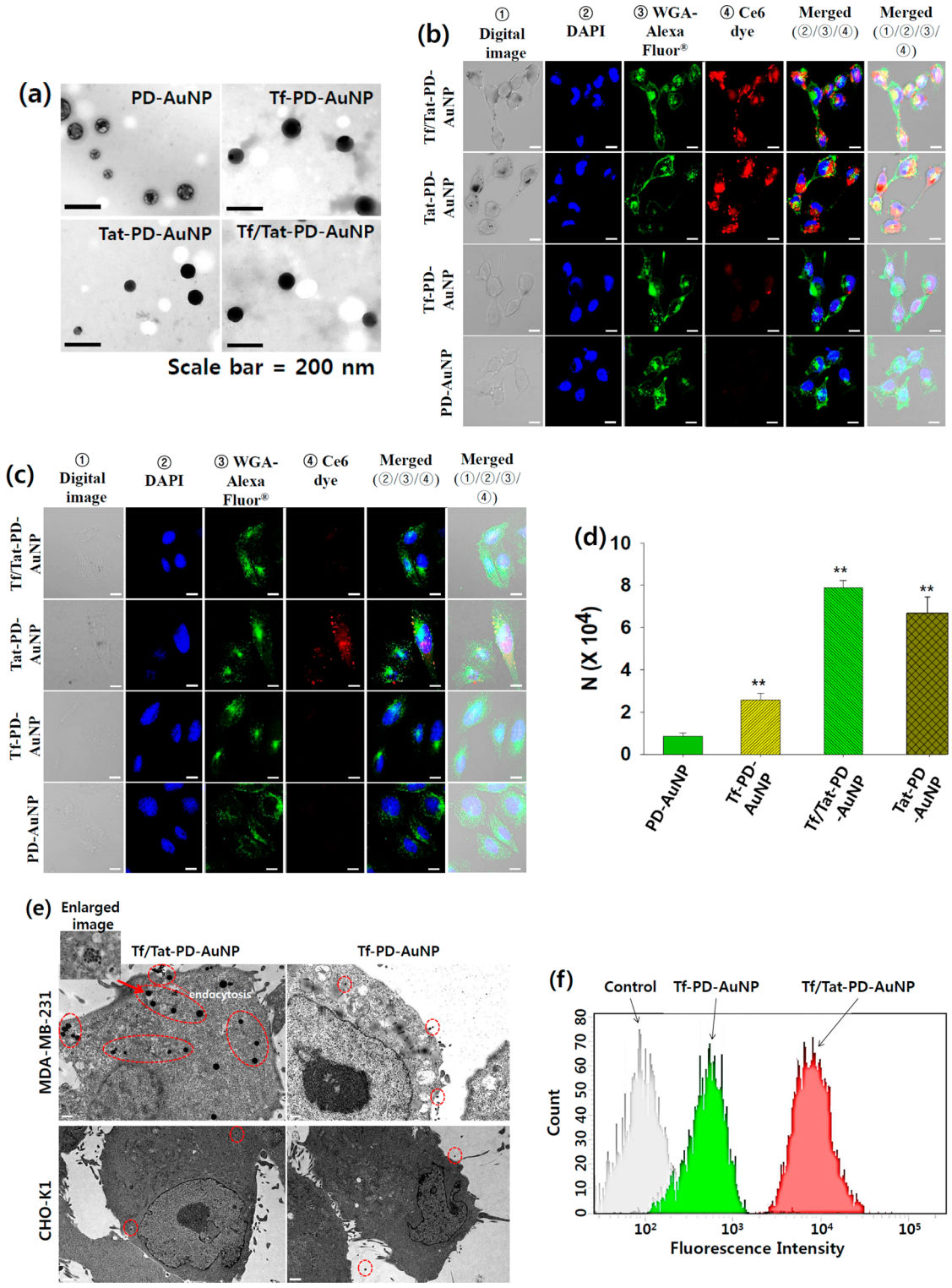

Figure 2. (a) TEM images of each AuNP. Confocal images (white scale bar = 10 μm) of (b) MDA-MB-231 (TfR-positive) and (c) CHO-K1 (TfR-negative) cells treated using fluorescent Ce6 dye-labeled AuNP (10 μg/mL) at 37 °C for 4 h. The treated cells were stained using DAPI and WGA-Alexa Fluor 488. (d) Uptake value [number (*N*) of AuNP taken up per the MDA-MB-231 cell] of each AuNP ($n = 7$) measured using an ICP-MS ($p < 0.01$ compared to the PD-AuNP). (e) TEM images of tumor cells treated with each AuNP (10 μg/mL) at 37 °C for 1 h (scale bar = 1 μm). (f) Flow cytometry analysis of Ce6 dye-labeled AuNP (10 μg/mL) for MDA-MB-231 tumor cells (4 h incubation at 37 °C).**

We further investigated the potential use of Tf/Tat-PD-AuNP *in vivo*. MDA-MB-231 tumor-bearing nude mice were selected as animal models. We administered fluorescent Ce6 dye-labeled AuNP to MDA-MB-231 tumor-bearing nude mice. Figure 3a shows typical serial near-infrared (NIR) photoluminescence images

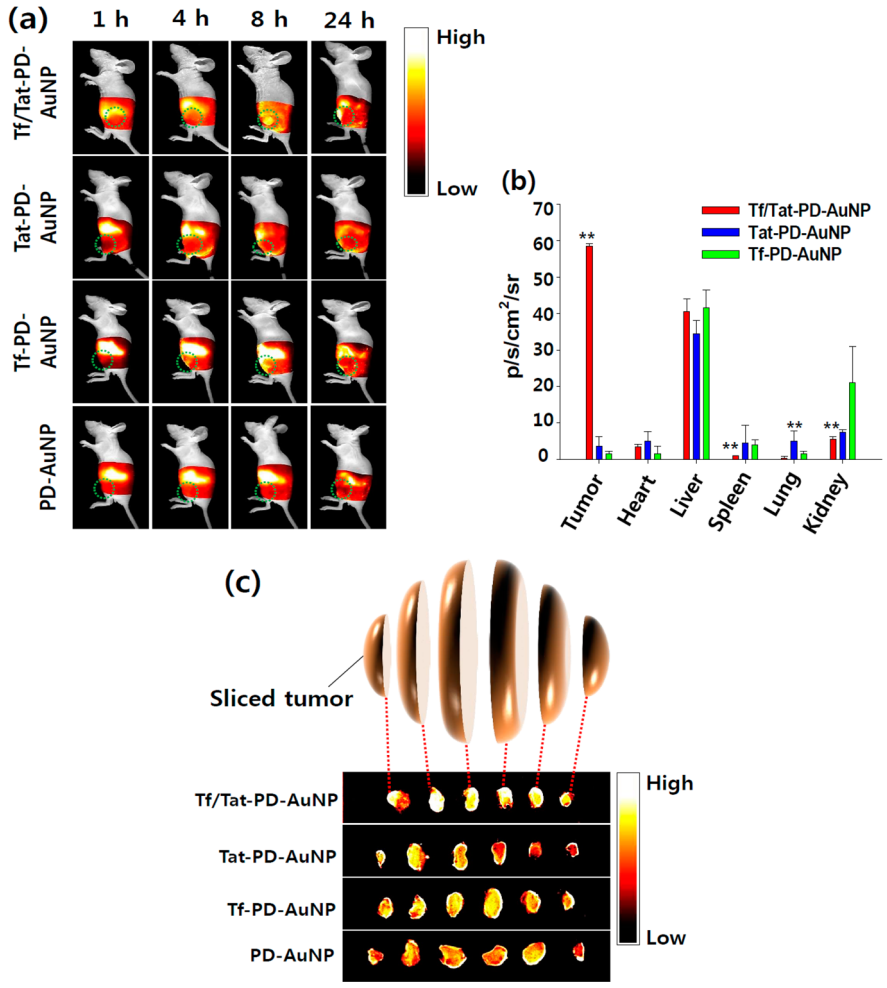

Figure 3. (a) *In vivo* noninvasive photoluminescent imaging of fluorescent Ce6 dye-labeled AuNP (2.5 mg/kg) injected intravenously into MDA-MB-231 tumor-bearing nude mice. Fluorescence images were obtained at 1, 4, 8, and 24 h postinjection. The tumor site is indicated by a dotted circle. (b) Total photon counts per centimeter squared per steradian (p/s/cm^2/sr, measured using an Image Station 4000 MM) of organs extracted (8 h postinjection) from MDA-MB-231 tumor-bearing nude mice injected with each AuNP (n = 3) (p < 0.01 compared to the Tf-PD-AuNP). (c) Fluorescence images of the sliced area of the *in vivo* tumor tissues extracted from MDA-MB-231 tumor-bearing nude mice (24 h postinjection of each AuNP).**

of the tumor-bearing nude mice obtained at 1, 4, 8, and 24 h postinjection. The use of nude mice injected with Tf/Tat-PD-AuNP allowed high-resolution fluorescent images to be taken of the *in vivo* tumor site, and the results were comparable to those observed with other AuNP. In particular, at 8 h postinjection of Tf/Tat-PD-AuNP, the NIR fluorescence was strongly detected in the tumor site. The nude mice were sacrificed at 8 h postinjection, and the excised organs (tumor, heart, liver, spleen, lung, and kidney) were analyzed. The total photon counts (fluorescence intensities) per centimeter squared per steradian (p/s/cm^2/sr)[19] per each excised tumor of tumor-bearing nude mice were 58 (Tf/Tat-PD-AuNP), 3 (Tat-PD-AuNP), and 2 (Tf-PD-AuNP) (Figure 3b). Tf/Tat-PD-AuNP effectively accumulated in the tumor tissue, although strong fluorescence was noted in the liver (indicating the nonspecific uptake of the nanoparticles by the reticuloendothelial system in the liver[5,20]). Furthermore, we evaluated the accumulation of AuNP in the interior tissue of the tumor by observing the fluorescence of the tumor tissues sliced using a microtome. The fluorescent image of sliced *in vivo* tumor tissues demonstrated that Tf/Tat-PD-AuNP facilitated the penetration of the interior tumor tissue, which is comparable with the results obtained after treatment with Tat-PD-AuNP, Tf-PD-AuNP, and PD-AuNP (Figure 3c).

Figure 4 shows the *in vivo* therapeutic efficiency of Tf/Tat-PD-AuNP in the MDA-MB-231 tumor-bearing nude mice model. It is known that AuNP convert light radiation to vibrational energy to elevate the ambient temperature.[7,21] In a preliminary study, Tf/Tat-PD-AuNP demonstrated a major increase (from 30 °C to 62 °C) in ambient temperature when the aqueous solution was irradiated at a light intensity of 1 W/cm^2 using an 808 nm laser source (Figure 4a), which is similar to that observed with Tat-PD-AuNP, Tf-PD-AuNP, and PD-AuNP (data not shown). For *in vivo* animal studies,

we administered Tf/Tat-PD-AuNP to tumor-bearing nude mice. At 8 h postinjection, the tumor sites of the tumor-bearing nude mice were locally irradiated once at a light intensity of 1 W/cm^2 using an 808 nm laser source for 6 min. After the light irradiation, thermal body images of the tumor-bearing nude mice were captured using a thermal imaging camera. The tumor surface temperature on the nude mice given Tf/Tat-PD-AuNP reached approximately 50 °C (Figure 4b). This hyperthermic condition[7] resulted in increased tumor volume regression in the nude mice (Figure 4c and d). The relative tumor volume in nude mice given Tf/Tat-PD-AuNP was approximately 7.1 times smaller than in those treated with PBS (control). Overall, these data indicate that the enhanced tumor uptake of Tf/Tat-PD-AuNP resulted in a significant improvement of *in vivo* tumor inhibition.

CONCLUSIONS

Based on the results of this study, we anticipate that this Y-shaped system will exhibit great potential as an advanced platform technology that can be coupled with various conventional ligands or antibodies for biomedical applications involving drug delivery and disease imaging.

MATERIALS AND METHODS

Materials. Cysteine, dicarboxylated poly(ethylene glycol) (HOOC-PEG-COOH) (M_n ~2 kDa), *N*-hydroxysuccinimide (NHS), *N*,*N*′-dicyclohexylcarbodiimide (DCC), transferrin (Tf), dopamine, dichloromethane (DCM), ethanol, anhydrous diethyl ether, triethylamine (TEA), *N*-(2-aminoethyl maleimide) (Mal), dimethyl sulfoxide (DMSO), dimethylformamide (DMF), $HAuCl_4$, tetraoctylammonium bromide, toluene, sodium borohydride, sulfuric acid, dodecanethiol, chloroform, 4′,6-diamidino-2-phenylindole dihydrochloride (DAPI), paraformaldehyde, glutaraldehyde, osmium tetroxide, HCl, Epon 812, and 1-ethyl-3-(3-(dimethylamino)-propyl)carbodiimide (EDC) were obtained from Sigma-Aldrich (USA). BCA protein assay kit was purchased from Pierce (USA). Tat peptide [Gly-Cys-$(Gly)_3$-Tyr-Gly-Arg-$(Lys)_2$-$(Arg)_2$-Gln-$(Arg)_3$][5] and fluorescein isothiocyanate (FITC)-conjugated Tat peptide[5] were obtained from Peptron Inc. (Republic of Korea). Fluorescent chlorin e6 (Ce6)[15] was purchased from Frontier Scientific Inc. (USA). RPMI-1640, fetal bovine serum (FBS), penicillin, and streptomycin were purchased from Welgene Inc. (South Korea). Wheat germ agglutinin Alexa Fluor 488 conjugate (WGA-Alexa Fluor 488) was purchased from Life Technologies (USA).

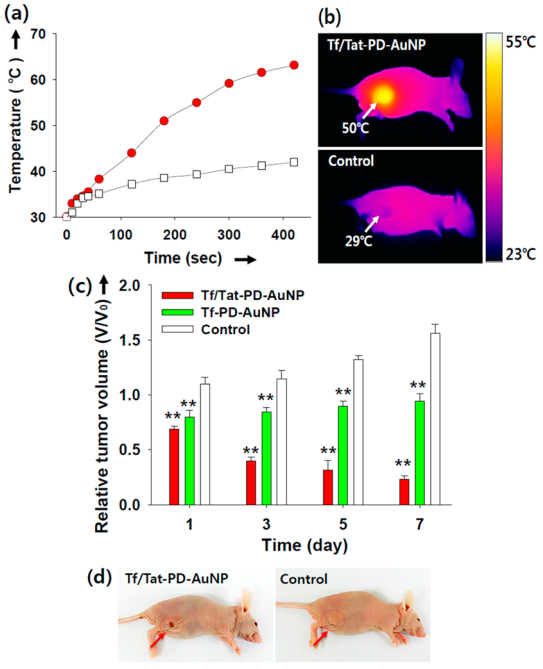

Figure 4. (a) Temperature change of 1 mL of phosphate-buffered saline (PBS, 150 mM, pH 7.4) with (●) or without (□) Tf/Tat-PD-AuNP (10 mg) irradiated at a light intensity of 1 W/cm^2 using an 808 nm laser source. (b) *In vivo* thermographic images of MDA-MB-231 tumor-bearing nude mice locally irradiated at a light intensity of 1 W/cm^2 using an 808 nm laser source for 6 min [8 h postinjection of each AuNP or control (PBS)]. (c) Relative tumor volume change (V/V_0, where V is the tumor volume at a given time, and V_0 is the initial tumor volume) of MDA-MB-231 tumor-bearing nude mice locally irradiated at 8 h postinjection of each AuNP or control (PBS) (n = 5) (p < 0.01 compared to the control). (d) Optical images of MDA-MB-231 tumor-bearing nude mice at 7 days postinjection.**

Synthesis of Y-Shaped PEG/Dopamine. To prepare the Y-shaped PEG, HOOC-PEG-COOH was preactivated using NHS and Mal. First, NHS-difunctionalized PEG (NHS-PEG-NHS)[17] was synthesized after the chemical reaction of HOOC-PEG-COOH (1 g) with DCC (400 mg) and NHS (340 mg) in DCM (20 mL) at 25 °C for 1 day. After the reaction, a drop of water was added to the solution to convert (unreacted) DCC to insoluble dicyclohexylurea (DCU). The solution was filtered and recrystallized after adding excess anhydrous diethyl ether. Next, Mal-difunctionalized PEG (Mal-PEG-Mal)[17] was prepared after the chemical reaction of NHS-PEG-NHS (1 g) with Mal (300 mg) in DMF (20 mL) containing TEA (1 mL) at 25 °C for 1 day. After the reaction, the solution was filtered and recrystallized after adding excess anhydrous diethyl ether. To further purify NHS-PEG-NHS or Mal-PEG-Mal, the polymer dissolved in fresh DMSO was dialyzed (Spectra/Por MWCO 1 kDa) against DMSO for 3 days to remove unreacted chemicals.[17−19] The dialyzed solution was lyophilized. The yields of NHS-PEG-NHS and Mal-PEG-Mal were 73 ± 5% and 67 ± 8%, respectively, calculated after lyophilization.

Cysteine (100 mg) was reacted with excess NHS-PEG-NHS (3 g) and Mal-PEG-Mal (3 g) in DMSO (18 mL)/ethanol (2 mL) at 25 °C for 3 days, producing the Y-shaped PEG (**I**, Figure 1b and Figure S1). The resulting solution was dialyzed (Spectra/Por MWCO 3.5 kDa) against fresh DMSO for 3 days to remove unreacted chemicals and then lyophilized. The obtained Y-shaped PEG (**I**, 500 mg) was reacted with dopamine (250 mg) in DMF (10 mL) containing TEA (1 mL) at 25 °C for 3 days, producing Y-shaped PEG/dopamine (PD, **II**, Figure S1). The solution was recrystallized after adding excess anhydrous diethyl ether, and the precipitates were harvested. To remove unreacted chemicals, the product dissolved in deoinized water was dialyzed again (Spectra/Por MWCO 3.5 kDa) and lyophilized. The yields of **I** and **II** were 63 ± 7% and 84 ± 5%, respectively, calculated after lyophilization. The chemical structure of the polymers (**I** and **II**) was analyzed using a Bruker 300 MHz NMR spectrometer (Bruker, Germany). The number-average molecular weight (M_n) and weight-average molecular weight (M_w) of polymers were determined using an HPLC system (Waters, USA) equipped with a 410 differential refractometer and a gel permeation chromatography (GPC) KF-804 or GPC KF-805 column (Shodex, Tokyo, Japan) at a flow rate of 1.0 mL/min with DMF as the mobile phase at room temperature.[20]

PD-AuNP Preparation. To prepare AuNP, $HAuCl_4$ (300 mg) dissolved in deionized water (30 mL) was vigorously mixed with tetraoctylammonium bromide (2 g) dissolved in toluene (80 mL)

for 2 h. After removing the water phase, 25 mL of aqueous sodium borohydride (0.4 M) was slowly added to the organic phase (toluene). After stirring the solution for 24 h, the organic phase was extracted and washed using 0.1 M sulfuric acid and then deionized water. The solution was mixed with excess dodecanethiol (2400 μL) for 2 h. The toluene in the solution was evaporated, which produced a dried powder. The obtained powder was dispersed in chloroform and ultracentifuged at 25 000 rpm for 10 min to separate AuNP from unreacted chemicals. Next, the dried precipitates were again dissolved in chloroform and added to a round-bottomed flask.[14] Subsequently, chloroform was removed using a rotary evaporator (EYELA, N-1000, Fisher Scientific Inc., USA) to form a thin film on the surface of the flask. The film was rehydrated in deionized water using a sonicator (60 Hz for 5 min) at 25 °C,[18,19] producing AuNP dispersed in deionized water.

Next, water-soluble PD (5 g) was mixed with AuNP (100 mg) dispersed in deionized water (100 mL) at 25 °C for 8 h. The concentration of PD bound on AuNP was calculated after measuring the weight of the dried precipitate (PD-AuNP) after ultracentrifugation of the AuNP solution at 25 000 rpm for 10 min. The yield of PD-AuNP was 70 ± 7%, calculated after lyophilization.

Tf-PD-AuNP Preparation. PD-AuNP (100 mg) was preactivated using DCC (50 mg) and NHS (50 mg) in DMSO (10 mL) at 25 °C for 1 day. After the reaction, the solution was dialyzed (Spectra/Por MWCO 1 kDa) against fresh DMSO for 3 days to remove unreacted chemicals. The dialyzed solution was ultracentifuged at 25 000 rpm for 10 min to precipitate PD-AuNP. Next, the preactivated PD-AuNP (10 mg) reacted with Tf (1 mg) in 10 mL of PBS (150 mM, pH 7.4) at 25 °C for 4 h, producing Tf-PD-AuNP. The Tf concentration in Tf-PD-AuNP was calculated by performing the BCA protein assay for free Tf remaining in the supernatant obtained after the ultracentrifugation of the AuNP solution (obtained immediately after the coupling reaction) at 25 000 rpm for 10 min. The yield of Tf-PD-AuNP was 75 ± 8%, calculated after lyophilization.

Tat-PD-AuNP Preparation. PD-AuNP (10 mg) in 10 mL of PBS (150 mM, pH 7.4) was mixed with Tat peptide (1 mg) or FITC-conjugated Tat peptide (1 mg) at 25 °C for 4 h, producing Tat-PD-AuNP. The Tat peptide concentration in Tat-PD-AuNP was calculated by measuring the fluorescence intensity of free FITC-conjugated Tat peptide remaining in the supernatant obtained after the ultracentrifugation of the AuNP solution (obtained immediately after the coupling reaction) at 25 000 rpm for 10 min. The yield of Tat-PD-AuNP was 78 ± 7%, calculated after lyophilization.

Tf/Tat-PD-AuNP Preparation. Tf-PD-AuNP (10 mg) in 10 mL of PBS (150 mM, pH 7.4) was mixed with Tat peptide (1 mg) or FITC-conjugated Tat peptide (1 mg) at 25 °C for 4 h (Figure 1b), producing Tf/Tat-PD-AuNP. The Tat peptide concentration in Tf/Tat-PD-AuNP was calculated by measuring the FITC fluorescence intensity of Tf/Tat-PD-AuNP. The yield of Tf/Tat-PD-AuNP was 64 ± 5%, calculated after lyophilization.

Characterization of AuNP. The particle size distribution of each AuNP (0.1 mg/mL) dispersed in 150 mM PBS (pH 7.4) was analyzed using a Zetasizer 3000 instrument (Malvern Instruments, USA) equipped with a He−Ne laser at a wavelength of 633 nm and a fixed scattering angle of 90°.[17] The zeta-potential change of each AuNP (0.1 mg/mL) dispersed in 150 mM PBS (pH 7.4) was measured with a Zetasizer 3000 (Malvern Instruments).[17] The morphology of each AuNP (10 μg/mL) was confirmed using a transmission electron microscope (JEM 1010, Japan).[17,20]

***In Vitro* Cell Uptake Studies.** Human breast adenocarcinoma MDA-MB-231 cells and Chinese hamster ovarian CHO-K1 cells (from the Korean Cell Line Bank) were maintained in RPMI-1640 medium with 1% penicillin−streptomycin and 10% FBS in a humidified standard incubator with a 5% CO_2 atmosphere at 37 °C. Prior to testing, cells (1×10^5 cells/mL) suspended in RPMI-1640 medium were seeded onto well plates and cultured for 24 h.[16]

The cells were incubated with fluorescent Ce6 dye-labeled AuNP (10 μg/mL) at 37 °C for 4 h. The fluorescence intensity was analyzed using a FACSCalibur flow cytometer (Becton Dickinson, USA).[16] Furthermore, the treated cells were stained using DAPI and WGA-Alexa Fluor 488 to visualize the cell nuclei and cell membranes.[17] The cells were washed three times with fresh PBS (pH 7.4) and then examined using a confocal laser-scanning microscope (CarlZeiss Meta LSM510, Germany).[17] In addition, fluorescent Ce6 dye-labeled AuNP were simply prepared by mixing 50 μg of Ce6−dopamine conjugate [prepared after the chemical reaction of the carboxylic acid of the fluorescent Ce6 dye (1 mg) and the free amine of dopamine (1 mg) in the presence of EDC (0.5 mg) and NHS (0.5 mg) in PBS (pH 7.4, 1 mL) for 8 h] with each AuNP (1 mg) in PBS (pH 7.4) at 25 °C for 2 h. The weight fraction of Ce6 dye embedded in each AuNP was 1.2%, calculated by measuring the fluorescence intensity of the free Ce6−dopamine conjugate remaining in the supernatant obtained after ultracentrifugation of the AuNP solution at 25 000 rpm for 10 min. The unreacted Ce6−dopamine conjugate was then removed after dialyzing (Spectra/Por MWCO 100 kDa) the solution against fresh PBS (150 mM, pH 7.4) for 4 h.

Next, cells treated with each AuNP (10 μg/mL) at 37 °C for 1 h were washed three times with fresh PBS and fixed in 4% paraformaldehyde/2.5% glutaraldehyde in 0.1 M PBS for overnight. After washing with 0.1 M PBS, the specimens were postfixed with 1% osmium tetroxide in PBS for 1 h. The specimens were dehydrated using pure ethanol and embedded in Epon 812 resin at 60 °C for 2 days. Ultrathin sections (60−80 nm) were sliced from embedded specimens using an ultramicrotome (Leica Ultracut UCT, Germany) and then mounted onto carbon-coated copper grids and examined using TEM (JEM 1010, Japan) operating at 60 kV with a CCD camera (SC1000 Orion, USA).[22]

To confirm the cellular uptake value [number (*N*) of AuNP taken up per cell] of each AuNP, MDA-MB-231 cells were incubated with each AuNP (10 μg/mL) at 37 °C for 4 h, washed three times with fresh PBS at 25 °C, and then mixed with 1% HCl solution (10 mL) at 80 °C for 1 h. The AuNP concentration in the treated cells was measured using an ICP-MS (ICAP Q, Thermo Scientific Inc., USA).[18]

Animal Care. The *in vivo* studies were conducted using 6- to 8-week-old female nude mice (BALB/c, nu/nu mice, Institute of Medical Science, Tokyo, Japan). The nude mice were maintained under the guidelines of an approved protocol from the Institutional Animal Care and Use Committee (IACUC) of the Catholic University of Korea (Republic of Korea).

***In Vivo* Uptake Studies.** To prepare *in vivo* xenografted tumors, MDA-MB-231 tumor cells (1×10^7 cells in PBS pH 7.4) were subcutaneously injected into female nude mice. When the tumor volume reached 50−100 mm^3, fluorescent Ce6 dye-labeled AuNP (2.5 mg/kg) were intravenously injected into the tumor-bearing nude mice through the tail vein. Fluorescence images were obtained at 1, 4, 8, and 24 h postinjection using an Image Station 4000 MM (Kodak, USA) with a special C-mount lens and a long-wave emission filter (Omega Optical, Brattleboro, VT, USA).[16,20] At 8 h postinjection, the nude mice were sacrificed, and the total photon counts per centimeter squared per steradian (p/s/cm^2/sr) in the excised organs (tumor, heart, liver, spleen, lung, and kidney) were determined using an Image Station 4000 MM.[19] In addition, the tumor tissues extracted (24 h postinjection) from the sacrificed nude mice were sliced using a microtome and analyzed using an Image Station 4000 MM.[16]

***In Vivo* Photothermal Tumor Therapy.** Before performing the *in vivo* tumor inhibition test, the temperature change in 1 mL of PBS (150 mM, pH 7.4) containing Tf/Tat-PD-AuNP (10 mg) was monitored using a probe-type thermometer (905-T1, Testo Inc., USA) when the aqueous solution was irradiated at a light intensity of 1 W/cm^2 using an 808 nm laser source for 420 s.

Next, each AuNP (2.5 mg/kg, without Ce6 dye) or PBS (control) was intravenously injected into MDA-MB-231 tumor-bearing nude mice through the tail vein. At 8 h postinjection, the tumor sites of the nude mice were locally irradiated at a light intensity of 1 W/cm^2 using an 808 nm laser source for 6 min. Thermal body images of the MDA-MB-231 tumor-bearing nude mice were captured using a thermal imaging camera (T335, FLIR Systems Inc., USA). The tumor volume was calculated using the

following formula: tumor volume = length × (width)^2/2.[16] The relative tumor volume change (V/V_0), where V is the tumor volume at a given time and V_0 is the initial tumor volume,[17] was plotted. In addition, the change in the body weight of the nude mice treated with each AuNP was negligible (data not shown), which indicates that each AuNP exerted no apparent toxicity throughout the body.

Statistical Evaluation. All of the results were analyzed via Student's *t* test or ANOVA at a significance level of $p < 0.01$ (**). The MINITAB release 14 statistical software program was used for all statistical analyses.[16,17]

Conflict of Interest: The authors declare no competing financial interest.

Supporting Information Available: ^{1}H NMR analysis and molecular weight determination of (**I**) Y-shaped PEG and (**II**) PD. Characterization data of Tf/Tat-PD-AuNP. This material is available free of charge *via* the Internet at http://pubs.acs.org.

Acknowledgment. This work was financially supported by Basic Science Research Program through the National Research Foundation of Korea (NRF) funded by the Ministry of Education (NRF-2013R1A1A2004375).

REFERENCES AND NOTES

1. Schrama, D.; Reisfeld, R. A.; Becker, J. C. Antibody Targeted Drugs as Cancer Therapeutics. *Nat. Rev. Drug Discovery* **2006**, *5*, 147–159.
2. Wang, X.; Li, S.; Shi, Y.; Chuan, X.; Li, J.; Zhong, T.; Zhang, H.; Dai, W.; He, B.; Zhang, Q. The Development of Site-Specific Drug Delivery Nanocarriers Based on Receptor Mediation. *J. Controlled Release* **2014**, *193*, 139–153.
3. Young, J. S.; Morshed, R. A.; Kim, J. W.; Balyasnikova, I. V.; Ahmed, A. U.; Lesniak, M. S. Advances in Stem Cells, Induced Pluripotent Stem Cells, and Engineered Cells: Delivery Vehicles for Anti-glioma Therapy. *Expert Opin. Drug Delivery* **2014**, *11*, 1733–1746.
4. Lee, E. S.; Na, K.; Bae, Y. H. Super pH-Sensitive Multifunctional Polymeric Micelle. *Nano Lett.* **2005**, *5*, 325–329.
5. Lee, E. S.; Gao, Z.; Bae, Y. H. Recent Progress in Tumor pH Targeting Nanotechnology. *J. Controlled Release* **2008**, *132*, 164–170.
6. Lee, E. S.; Kim, D.; Youn, Y. S.; Oh, K. T.; Bae, Y. H. A Virus-Mimetic Nanogel Vehicle. *Angew. Chem., Int. Ed.* **2008**, *47*, 2418–2421.
7. Jang, B.; Park, J. Y.; Tung, C. H.; Kim, I. H.; Choi, Y. Gold Nanorod-Photosensitizer Complex for Near-Infrared Fluorescence Imaging and Photodynamic/Photothermal Therapy *in Vivo*. *ACS Nano* **2011**, *5*, 1086–1094.
8. Qiu, X.; Wang, H.; Cai, B.; Wang, L. L.; Yue, S. T. Small Antibody Mimetics Comprising Two Complementarity-Determining Regions and a Framework Region for Tumor Targeting. *Nat. Biotechnol.* **2007**, *25*, 921–929.
9. Derda, R.; Tang, S. K.; Li, S. C.; Ng, S.; Matochko, W.; Jafrai, M. R. Diversity of Phage-Displayed Libraries of Peptides during Panning and Amplification. *Molecules* **2011**, *16*, 1776–1803.
10. Firer, M. A. Antibody-Drug Conjugates in Cancer Therapy-Filling in the Potholes That Lie Ahead. *OA Cancer* **2013**, *1*, 8.
11. Jian, J.; Yang, Q.; Huang, X. Src Regulates Tyr(20) Phosphorylation of Transferrin Receptor-1 and Potentiates Breast Cancer Cell Survival. *J. Biol. Chem.* **2011**, *286*, 35708–35715.
12. Wadia, J. S.; Stan, R. V.; Dowdy, S. F. Transducible TAT-HA Fusogenic Peptide Enhances Escape of TAT-Fusion Proteins after Lipid Raft Macropinocytosis. *Nat. Med.* **2004**, *10*, 310–315.
13. Fabregat, G.; Estrany, F.; Casas, M. T.; Aleman, C.; Armelin, E. Detection of Dopamine Using Chemically Synthesized Multilayered Hollow Microspheres. *J. Phys. Chem. B* **2014**, *118*, 4702–4709.
14. Barbe, K.; Kind, M.; Pfeiffer, C.; Terfort, A. Purification of Ethanol for Highly Sensitive Self-Assembly Experiments. *Beilstein J. Nanotechnol.* **2014**, *5*, 1254–1260.
15. Kakimoto, S.; Moriyama, T.; Tanabe, T.; Shinkai, S.; Nagasaki, T. Dual-Ligand Effect of Transferrin and Transforming Growth Factor Alpha on Polyethyleneimine-Mediated Gene Delivery. *J. Controlled Release* **2007**, *120*, 242–249.
16. Park, S. Y.; Baik, H. J.; Oh, Y. T.; Oh, K. T.; Youn, Y. S.; Lee, E. S. A Smart Polysaccharide/Drug Conjugate for Photodynamic Therapy. *Angew. Chem., Int. Ed.* **2011**, *50*, 1644–1647.
17. Lee, U. Y.; Oh, Y. T.; Kim, D.; Lee, E. S. Multimeric Grain-Marked Micelles for Highly Efficient Photodynamic Therapy and Magnetic Resonance Imaging of Tumors. *Int. J. Pharm.* **2014**, *471*, 166–172.
18. Cho, E. C.; Liu, Y.; Xia, Y. A Simple Spectroscopic Method for Differentiating Cellular Uptakes of Gold Nanospheres and Nanorods from Their Mixtures. *Angew. Chem., Int. Ed.* **2010**, *49*, 1976–1980.
19. Kwag, D. S.; Oh, K. T.; Lee, E. S. Facile Synthesis of Multi-layered Polysaccharidic Vesicles. *J. Controlled Release* **2014**, *187*, 83–90.
20. Lee, J. O.; Oh, K. T.; Kim, D.; Lee, E. S. pH-Sensitive Short Worm-Like Micelles Targeting Tumors Based on the Extracellular pH. *J. Mater. Chem. B* **2014**, *2*, 6363–6370.
21. Cheng, L.; Wang, C.; Feng, L.; Yang, K.; Liu, Z. Functional Nanomaterials for Phototherapies of Cancer. *Chem. Rev.* **2014**, *114*, 10869–10939.
22. Kwag, D. S.; Park, K.; Oh, K. T.; Lee, E. S. Hyaluronated Fullerenes with Photoluminescent and Antitumoral Activity. *Chem. Commun.* **2013**, *49*, 282–284.